Exploring Lightning Jump Characteristics

Article *in* Weather and Forecasting · February 2015

DOI: 10.1175/WAF-D-14-00064.1

CITATIONS
52

READS
509

6 authors, including:

Themis Chronis
University of Alabama in Huntsville
61 PUBLICATIONS **1,279** CITATIONS
SEE PROFILE

Lawrence Carey
University of Alabama in Huntsville
152 PUBLICATIONS **4,574** CITATIONS
SEE PROFILE

Elise V Schultz
CFD Research Corporation
15 PUBLICATIONS **440** CITATIONS
SEE PROFILE

Kristin Calhoun
National Oceanic and Atmospheric Administration
51 PUBLICATIONS **1,310** CITATIONS
SEE PROFILE

Exploring Lightning Jump Characteristics

T. CHRONIS,* LAWRENCE D. CAREY,+ CHRISTOPHER J. SCHULTZ,# ELISE V. SCHULTZ,* KRISTIN M. CALHOUN,@ AND STEVEN J. GOODMAN&

*Earth System Science Center, University of Alabama in Huntsville, Huntsville, Alabama
+Department of Atmospheric Science, University of Alabama in Huntsville, Huntsville, Alabama
#Department of Atmospheric Science, University of Alabama in Huntsville, and NASA Marshall Space Flight Center, Huntsville, Alabama
@Cooperative Institute for Mesoscale Meteorology Studies, Oklahoma University, and National Severe Storms Laboratory, Norman, Oklahoma
&NOAA/National Environmental Satellite, Data, and Information Service, Greenbelt, Maryland

(Manuscript received 13 June 2014, in final form 17 November 2014)

ABSTRACT

This study is concerned with the characteristics of storms exhibiting an abrupt temporal increase in the total lightning flash rate [i.e., lightning jump (LJ)]. An automated storm tracking method is used to identify storm ''clusters'' and total lightning activity from three different lightning detection systems over Oklahoma, northern Alabama, and Washington, D.C. On average and for different employed thresholds, the clusters that encompass at least one LJ (LJ1) last longer and relate to higher maximum expected size of hail, vertical integrated liquid, and lightning flash rates (area normalized) than do the clusters without an LJ (LJ0). The respective mean radar-derived and lightning values for LJ1 (LJ0) clusters are 80 min (35 min), 14 mm (8 mm), 25 kg m^{-2} (18 kg m^{-2}), and 0.05 flash min^{-1} km^{-2} (0.01 flash min^{-1} km^{-2}). Furthermore, the LJ1 clusters are also characterized by slower-decaying autocorrelation functions, a result that implies a less ''random'' behavior in the temporal flash rate evolution. In addition, the temporal occurrence of the last LJ provides an estimate of the time remaining to the storm's dissipation. Depending on the LJ strength (i.e., varying thresholds), these values typically range between 20 and 60 min, with stronger jumps indicating more time until storm decay. This study's results support the hypothesis that the LJ is a proxy for the storm's kinematic and microphysical state rather than a coincidental value.

1. Introduction

The advent of ground-based lightning detection networks in recent decades has made real-time retrieval of total lightning activity [cloud to ground (CG) and intracloud (IC)] available in both high spatial and temporal resolutions. Although there are uncertainties in the details (Takahashi 1978; Saunders 1993), it is known that rebounding collisions between graupel and ice crystals in the presence of supercooled water is the primary process for thunderstorm electrification (MacGorman and Morgenstern 1998; Saunders et al. 2006; Emersic and Saunders 2010). Several studies have documented a temporal covariability between updraft mass flux, precipitation ice mass, and overall storm depth with the respective total lightning activity (e.g., Goodman et al. 1988; Carey and Rutledge 2000; Chronis et al. 2007; Deierling and Petersen 2008; Bruning and MacGorman 2013). Hence, it would be reasonable to suggest that an abrupt temporal change on the order of a few minutes in the total lightning activity is considered to be a severe weather indicator [lightning jump (LJ); see Schultz et al. (2009), (2011)]. Studies by Williams et al. (1999), Gatlin and Goodman (2010), Carey et al. (2009), Schultz et al. (2009, 2011), and Rudlosky and Fuelberg (2013) document that statistics such as lead time, probability of detection, and false alarm ratio could be improved based on the use of total lightning as a metric for storm intensity. Nonetheless, these methods can be hindered by problems related to uncertainties in severe weather observations at the surface (Trapp et al. 2006; Keene et al. 2008; Schultz et al. 2011). This study puts forward an

Corresponding author address: Themis Chronis, Earth System Science Center, University of Alabama in Huntsville, 320 Sparkman Dr., Huntsville, AL 35805.
E-mail: themis.chronis@nsstc.uah.edu

DOI: 10.1175/WAF-D-14-00064.1

original comparison between the convective characteristics of storms that did or did not exhibit an LJ throughout their lifetime. This evaluation relies on radar-derived and lightning properties.

2. Data and methods

a. Storm tracking and clustering

The storm identification and tracking have been performed in real time utilizing the Warning Decision Support System–Integrated Information (WDSS-II; Lakshmanan et al. 2007). A storm "cluster" is automatically identified by the reflectivity across the −10°C isothermal layer, following a merger of individual WSR-88D. A combination of watershed segmentation and *k*-means clustering is employed to identify the storm clusters (Lakshmanan et al. 2009; Kolodziej Hobson et al. 2012; Cintineo et al. 2014). To complete the storm identification, the algorithm searches for local reflectivity Z maxima where $Z > 20$ dBZ, then incrementally grows the area until it is at least 200 km^2. The storm cluster is then matched with a separately identified cluster at the next time step (for our analysis, a 1-min time step was employed) using a cost function, where longer-lived cells are given preference in the case of storm mergers.

Each storm (hereinafter cluster) is described by a geolocated polygon (i.e., footprint). The lifespan is determined by the total time a cluster was tracked by WDSS-II (Lakshmanan and Smith 2009). The maximum vertical integrated liquid (VIL; Greene and Clark 1972) and the maximum expected size of hail (MESH; Witt et al. 1998; Cintineo et al. 2012) are retrieved for each cluster for the duration of its lifetime. Both VIL and MESH have been used as radar-derived intensity metrics for storm properties such as liquid precipitation, updraft strength, and hail growth (Amburn and Wolf 1996; Witt et al. 1998). As with any proxy, there are caveats that reflect the imperfect representations of severe weather potential and these emanate from parameters unrelated to the storm dynamics [e.g., distance from the radar, tilted updrafts, storm speed, etc.; Stumpf et al. (2004)]. To mitigate these effects as much as possible, all available radars in the area are used to retrieve these proxies. Five radars over each of the three locations are employed, namely, KFDR, KTLX, KVNX, KINX, and KSRX for Oklahoma; KHTX, KGWX, KBMX, KOHX, and KFFC for northern Alabama; and KLWX, KDOX, KAKQ, KCCX, and KDIX for Washington, D.C. (Table 1; https://www.ncdc.noaa.gov/nexradinv/map.jsp). The data for the present study extend from 1 April through 14 August 2013.

TABLE 1. Acronym and expansion of radars.

Acronym	Expansion
Oklahoma	
KFDR	Altus Air Force Base, Oklahoma
KTLX	Oklahoma City, Oklahoma
KVNX	Vance Air Force Base, Oklahoma
KINX	Tulsa, Oklahoma
KSRX	Fort Smith, Arkansas
Northern Alabama	
KHTX	Huntsville, Alabama
KGWX	Columbus Air Force Base, Mississippi
KBMX	Birmingham, Alabama
KOHX	Nashville, Tennessee
KFFC	Atlanta, Georgia
Washington, D.C.	
KLWX	Sterling, Virginia
KDOX	Dover Air Force Base, Delaware
KAKQ	Norfolk/Rich, Virginia
KCCX	State College, Pennsylvania
KDIX	Philadelphia, Pennsylvania

b. Total lightning activity and the lightning jump algorithm

This study employs three total lightning detection networks: 1) the Lightning Mapping Array (LMA) networks located in central/southwestern Oklahoma (MacGorman et al. 2008), northern Alabama (Goodman et al. 2005), and Washington, D.C. (Krehbiel 2008); 2) the Earth Networks Total Lightning Network (ENTLN; Liu and Heckman 2011); and 3) the National Lightning Detection Network (NLDN; Cummins et al. 1995, 2006; Cummins and Murphy 2009).

The LMA detects the very high-frequency (VHF) radiation emitted during the elemental processes that compose a lightning discharge [e.g., the initial breakdown, leader propagation, and other *K* processes; Uman (1987)] with a location accuracy measured in tens of meters and with a time resolution of 80–100 μs (Thomas et al. 2004). Both IC and CG flashes are detected although the distinction can be dubious because of limitations in range. The location accuracy is also range dependent; however, it is relatively constant to a ~150-km radius from the respective center (Thomas et al. 2004; Koshak et al. 2004). The following analysis relies on the total lightning flashes occurring within ~120 km of the respective LMA center (Thomas et al. 2003). Lightning flashes are retrieved from the LMAs via grouping at least 10 detected VHF radiation sources, using time and space constraints (3 km and 150 ms) between the adjoining points (McCaul et al. 2005). Only flashes that begin within the storm cluster's footprint are counted toward the total flash rate. No classification between CG and IC flashes is performed using LMA data.

The ENTLN sensors operate over a wide frequency range, spanning from 1 Hz to 12 MHz. According to Liu and Heckman (2011), electric field waveforms are used in locating as well as classifying the IC and CG flashes. Multiple strokes (or individual cloud events) are clustered into a single flash if they are within 700 ms and 10 km of the first detected stroke. A flash that contains at least one return stroke is classified as a CG flash; otherwise, it is classified as an IC flash.

Since the late 1980s, the NLDN has served as the source for many CG lightning-related studies over the United States. The network consists of 113 sensors that combine the advantages of direction finding and time-of-arrival techniques. The NLDN CG detection efficiency ranges between 90% and 95% over the midlatitude continental United States, with a median location error of better than 500 m (Cummins and Murphy 2009; Rudlosky and Fuelberg 2010). Although the NLDN is designed to primarily detect CG flashes, it has been recently reported that IC flashes are also detected, depending on the restrictions applied to the processed waveforms [peak-to-zero rise time; Murphy and Nag (2014)].

The present study employs the total flash activity (IC and CG) for all lightning detection systems. Rudlosky and Fuelberg (2013) use a similar methodology for compiling lightning and radar data. Both NLDN and ENTLN have national (U.S.) coverage. Nevertheless, for this analysis the respective total lightning activity is computed only for the clusters that are identified over a radius around where the optimum LMA operation is ensured. Further detailed comparison (e.g., relative location accuracy and detection efficiency) between the lightning detection systems lies outside the scope of this paper. However, their employment is considered as a preliminary attempt to demonstrate results pertaining to the LJ properties from lightning detection networks of different technical specifications (e.g., detection efficiency).

The 1-min flash rate is computed by adding all the flashes occurring within the footprint of the identified cluster. The LJ is objectively identified by Schultz et al. (2009, 2011). This technique uses 14 min of the cluster's most recent flash rate history. Twelve of the 14 min are considered to calculate the minimum jump threshold that must be exceeded for an LJ to occur. The remaining 2 min are used to determine whether the current rate of change in the total flash rate exceeds the LJ threshold. As outlined in Schultz et al. (2009, 2011), the algorithm is a five-step process. These steps are as follows. 1) The total flash rate (flashes min^{-1}) from the 14-min period is binned into 2-min segments and the total flash rate is averaged:

$$\text{FR}_{\text{avg}}(t) = \frac{\text{FR}(t) + \text{FR}(t-1)}{2}. \quad (1)$$

2) The rate of change of the total flash rate (DFRDT; flashes min^{-2}) is calculated by subtracting consecutive bins from each other:

$$\frac{d}{dt}\text{FR}_{\text{avg}}(t) = \frac{\text{FR}_{\text{avg}}(t) - \text{FR}_{\text{avg}}(t-1)}{2} = \text{DFRFT}. \quad (2)$$

This results in six DFRDT values (flashes min^{-2}). 3) The five earliest DFRDT values in time are used to calculate the standard deviation σ of the population. 4) If DFRDT $> \alpha\sigma$ and the flash rate is greater than a given flash rate threshold (FRT), then an LJ has occurred. Note that α represents a multiplicative factor and has no relation to the standard deviation. In the original studies by Schultz et al. (2009, 2011), α and FRT were set to 2.0 and 10 flashes min^{-1}, respectively. Also note that α is dimensionless (i.e., flashes min^{-2}/flashes min^{-2}). Here, we compute the LJ based on a variable α (0.5–4; step of 0.5) and FRT (5–25 flashes min^{-1}; step of 5 flashes min^{-1}). The latter is employed in order to define the LJ relative strength. For example, a weaker LJ1 would have $\alpha = 1.0$ and FRT = 10 flashes min^{-1}, while a stronger LJ1 would be considered to be $\alpha = 2.0$ and FRT = 15 flashes min^{-1}. 5) This process is repeated every 2 min as new total lightning flash rates are collected until the storm dissipates.

We note that the above-implemented time window within which we calculate the LJ based on empirical observations of the growth and decay on the convective time scale (<10–20 min). Had we allowed for longer periods (e.g., 40–60 min) into the thunderstorm's lifetime, we would likely have missed the occurrence of the first LJ and a potentially severe weather occurrence. This is why we have empirically tested this algorithm with over 700 storms in multiple storm environments to help understand the variability of the algorithm (Schultz et al. 2011). The choice of the 2σ (i.e., $\alpha = 2$) in Schultz et al. (2011) is simply a benchmark to which this study is not tied.

3. Analysis and discussion

a. Data and quality control

As WDSS-II tracks cluster independently of the respective total lightning activity, the number of the identified LJ0 and LJ1 clusters is considerably different. For instance, more than 2000 clusters are classified as LJ0 at $\alpha = 2.0$ and FRT = 10 flashes min^{-1}, whereas less than 200 are classified as LJ1 for the same α and FRT values. To ensure a comparable sample size and to

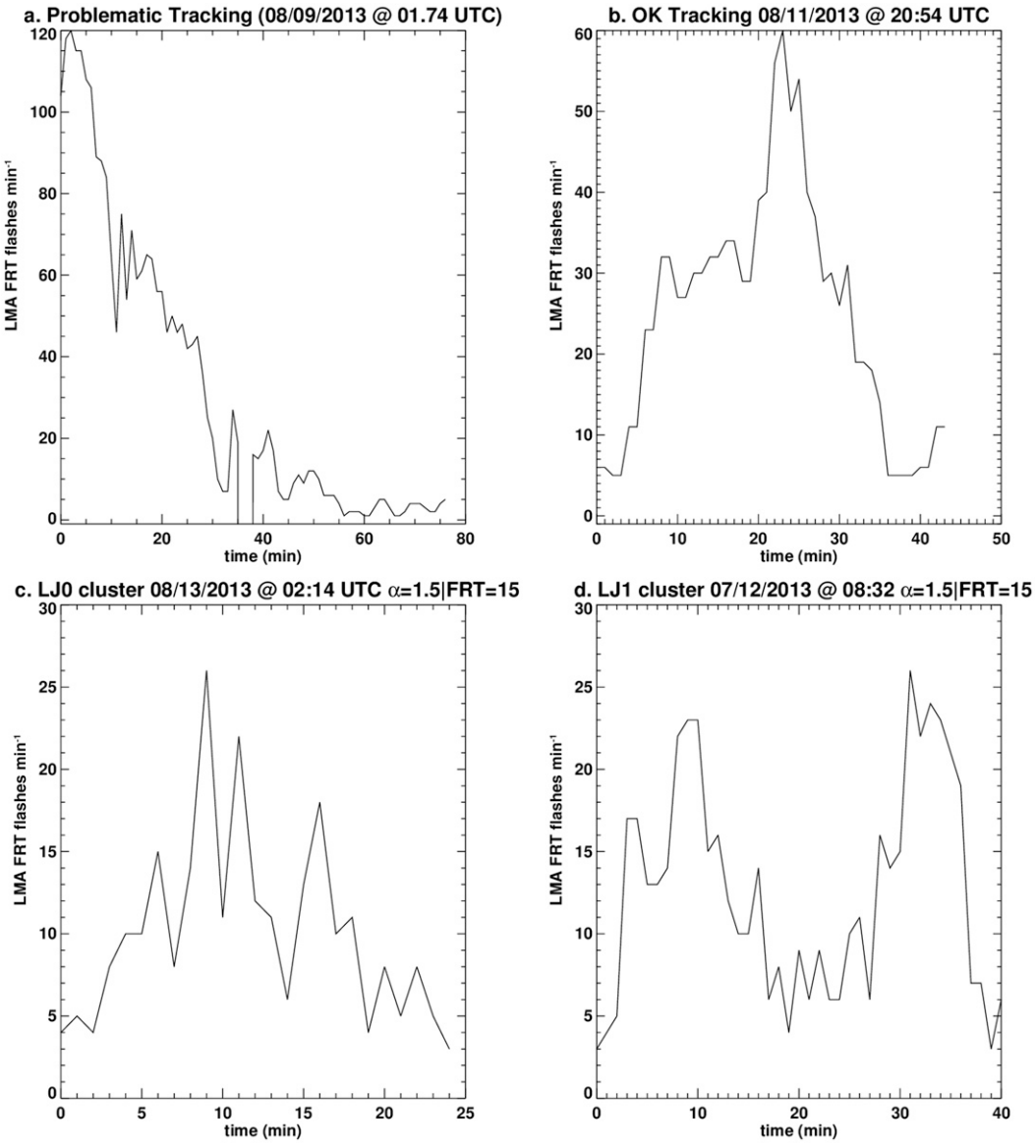

FIG. 1. Tracked cluster that exhibits (a) problematic tracking (e.g., cluster entering the area with already high flash rates) and (b) normal tracking (i.e., complies with both QC1 and QC2). (c) LJ0 and (d) LJ1 clusters of comparable flash rates.

improve the representativeness of the data, we report on the LJ0 and LJ1 clusters that exhibit sustained total lightning activity for more than 95% during their life span (e.g., if a cluster is tracked for 100 min, the cluster must exhibit total lightning activity greater than zero for at least 95 min). This quality constraint (QC1) may classify a slightly different number of clusters depending on the employed lightning detection system. An additional quality constraint (QC2) is applied to the clusters that start or end at a flash rate that is notably higher than zero (set to >10 flashes min^{-1}). Typically, these cases represent merging or splitting clusters or clusters that entered/exited the effective radius of the LMA with high flash rates. QC2 also takes care of potential problems with MESH/VIL repetitiveness due to distance from the radar. Given that the study explores aspects such as the storm duration, the clusters that failed to conform to QC2 are omitted from the analysis. Examples from a tracked cluster that exhibits a problematic tracking (e.g., cluster entering the area with already high flash rates), a normal tracking (i.e., complies with both QC1 and QC2), and an LJ0 cluster and an LJ1 cluster of comparable flash rates are shown in Figs. 1a–d, respectively.

All three lightning detection systems indicate that the number of LJ1 clusters decreases as the α and FRT values increase (i.e., fewer clusters at higher α and FRT values; Figs. 2b,d,f). Unlike the LJ1, the number of tracked LJ0 clusters increases as the values of α and FRT increase (Figs. 2a,c,e). The latter result should be expected since an LJ0 at, for example, $\alpha = 2.0$ and FRT = 10 flashes min^{-1} will also not exhibit LJs at higher α or FRT values.

b. *The autocorrelation function of LJ0 and LJ1 flash time series*

Autocorrelation is an essential tool for describing the independence of sequential values in a time series. A slow (fast)-decaying autocorrelation function with time (i.e., lag) indicates a consistent (random) pattern of behavior of the variable under consideration (Bowerman and O'Connell 1979). For example, a slow-decaying autocorrelation function of lightning activity time series would signal coherent behavior in the storm's updraft speed and volume (e.g., Schultz et al. 2009, 2011, 2014). Consequently, autocorrelation can elaborate on whether the presence of an LJ relates to a numerically random increase in the total lightning activity or points to a more persistent feature of the storm's dynamical evolution. The autocorrelation function is computed for the flash rates of LJ0 and LJ1, by introducing a time lag that ranges from 1 to $+N/2$ min, where N is the number of 1-min intervals during which the cluster is tracked (i.e., life span). The lag at which the Pearson correlation is reduced below the 95% significance level denotes the e-folding time. Figure 3 illustrates the average e-folding times for the LJ0 and LJ1 clusters for different α and FRT values. The corresponding results (Fig. 3) show longer e-folding times for the LJ1 clusters. For example, the e-folding times for the LJ1 at $\alpha = 2.0$ and FRT = 15 flashes min^{-1} are computed as ~12 min for LMA, 12.7 min for the ENTLN, and 11.5 min for the NLDN. Conversely, the e-folding times for the LJ0 for the same α and FRT values are consistently less than ~4.0 min for all three lightning detection systems and any given α and FRT value. Moreover, the fact that the e-folding times for LJ1 clusters increase as both α and FRT values also increase illustrates a key observation that emphasizes the nonredundant numerical role of both variables α and FRT in the LJ algorithmic implementation (Schultz et al. 2009, 2011).

c. *Comparison of storm severity potential and physical characteristics between the LJ0 and LJ1 clusters*

The previous section studied the LJ0 and LJ1 clusters exclusively from the viewpoint of the flash rate temporal variation. This section explores the mean values of storm attributes derived from WDSS-II. As Fig. 4 demonstrates, the LJ1 clusters exhibit a longer life span than do the respective LJ0 cases, and this observation is consistent throughout the three lightning detection systems and all α and FRT values. For example, for $\alpha = 2.0$ and FRT = 15 flashes min^{-1}, the average life span is 80 min, whereas the respective LJ0 life span is approximately 35 min. Similar behavior is evident for the mean flash rate (normalized by the cluster's footprint area; flashes min^{-1} km^{-2}; Fig. 5), MESH (Fig. 6), and VIL (Fig. 7) values.

In particular, Fig. 5 indicates that on average, the LJ1 clusters exhibit ~4–5 times higher flash rates than do the respective LJ0 cases. For instance, the average LJ1 flash rates for $\alpha = 2.0$ and FRT = 15 flashes min^{-1} are ~0.054 flashes min^{-1} km^{-2} as opposed to ~0.015 flashes min^{-1} km^{-2} for the LJ0, an observation that is also consistent across all networks. In turn, the MESH values for the LJ1 clusters range from ~11 to 18 mm whereas the corresponding LJ0 values range from ~6.5 to 10 mm (Fig. 6). Likewise, the mean values of VIL are ~18 kg m^{-2} for the LJ0 clusters and ~25 kg m^{-2} for the respective LJ1 cases (Fig. 7). As is also highlighted in section 3b, higher flash rates and larger MESH and VIL values (Figs. 5–7) are found with increasing α and FRT thresholds. One could argue that it would be expected to have higher magnitudes of weather severity proxies (e.g., MESH, VIL, etc.) with higher flash rates. Nevertheless, the previous results also suggest that it is not only the flash rate (i.e., FRT) that exhibits a fundamental physical link to storm intensity but also its temporal evolution (i.e., α). The above results are also in agreement with the findings by Rudlosky and Fuelberg (2013).

d. *LJ strength and storm decay time*

The results shown in Fig. 4 support that the LJ1 clusters with larger α and FRT relate to storms with longer durations (Fig. 4). Approaching the latter from a different perspective, one can raise the following question: Does the strength of the final LJ occurrence relate to the remaining life span of the cluster? To address the above, we compute the time elapsed from the last LJ occurrence to the last time step that a cluster is tracked. Arguably, the results in Fig. 8 corroborate that both α and FRT play a role in the storm's remaining duration, which shows to increase from around 30–35 min for LJ1 of $\alpha = 1.0$ and FRT = 10 flashes min^{-1} to over 45–60 min for higher α and/or FRT values.

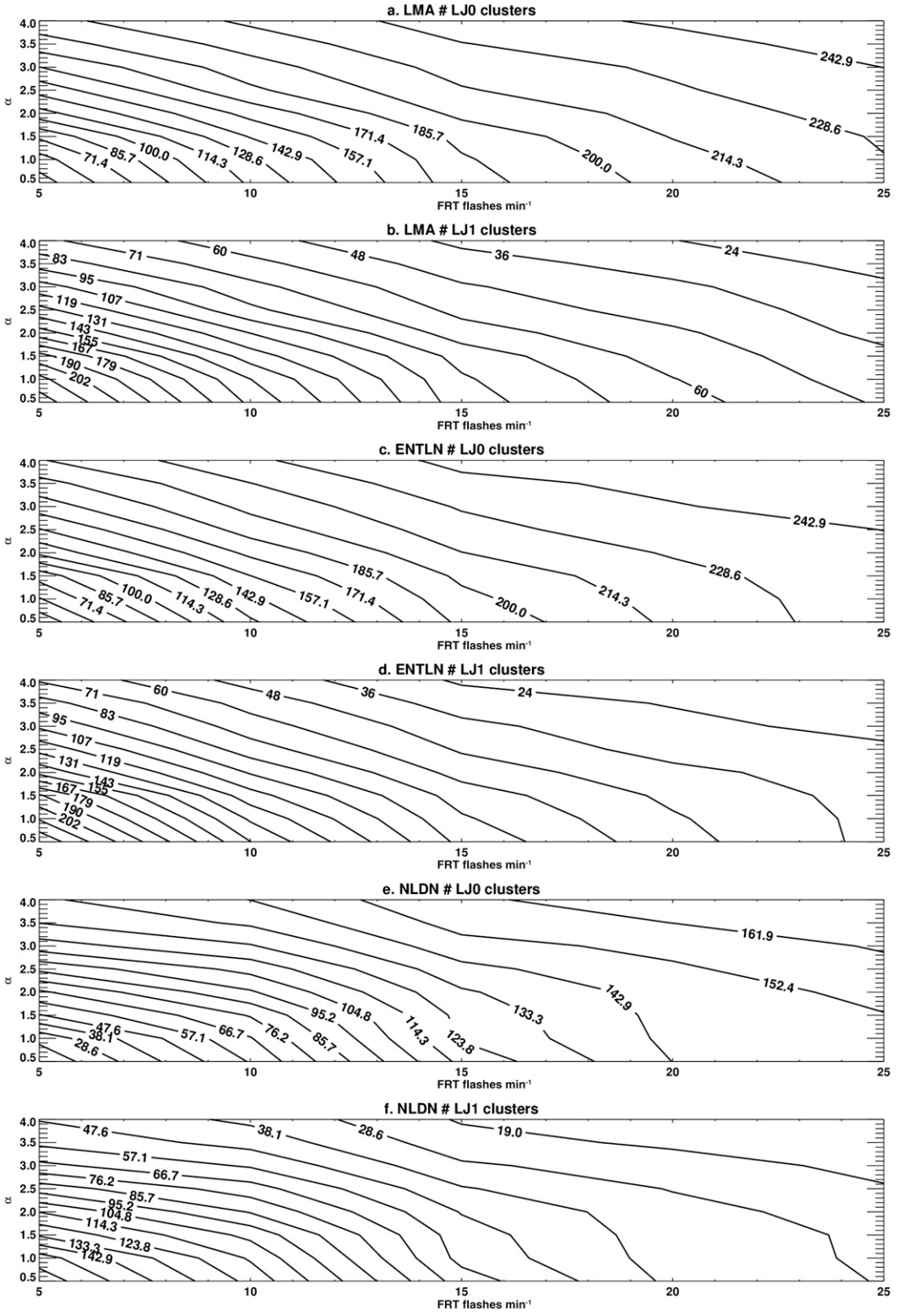

FIG. 2. The identified number of LJ0/LJ1 clusters as a function of FRT (x axis; flashes min^{-1}) and α (y axis) for (a),(b) LMA; (c),(d) ENTLN; and (e),(f) NLDN.

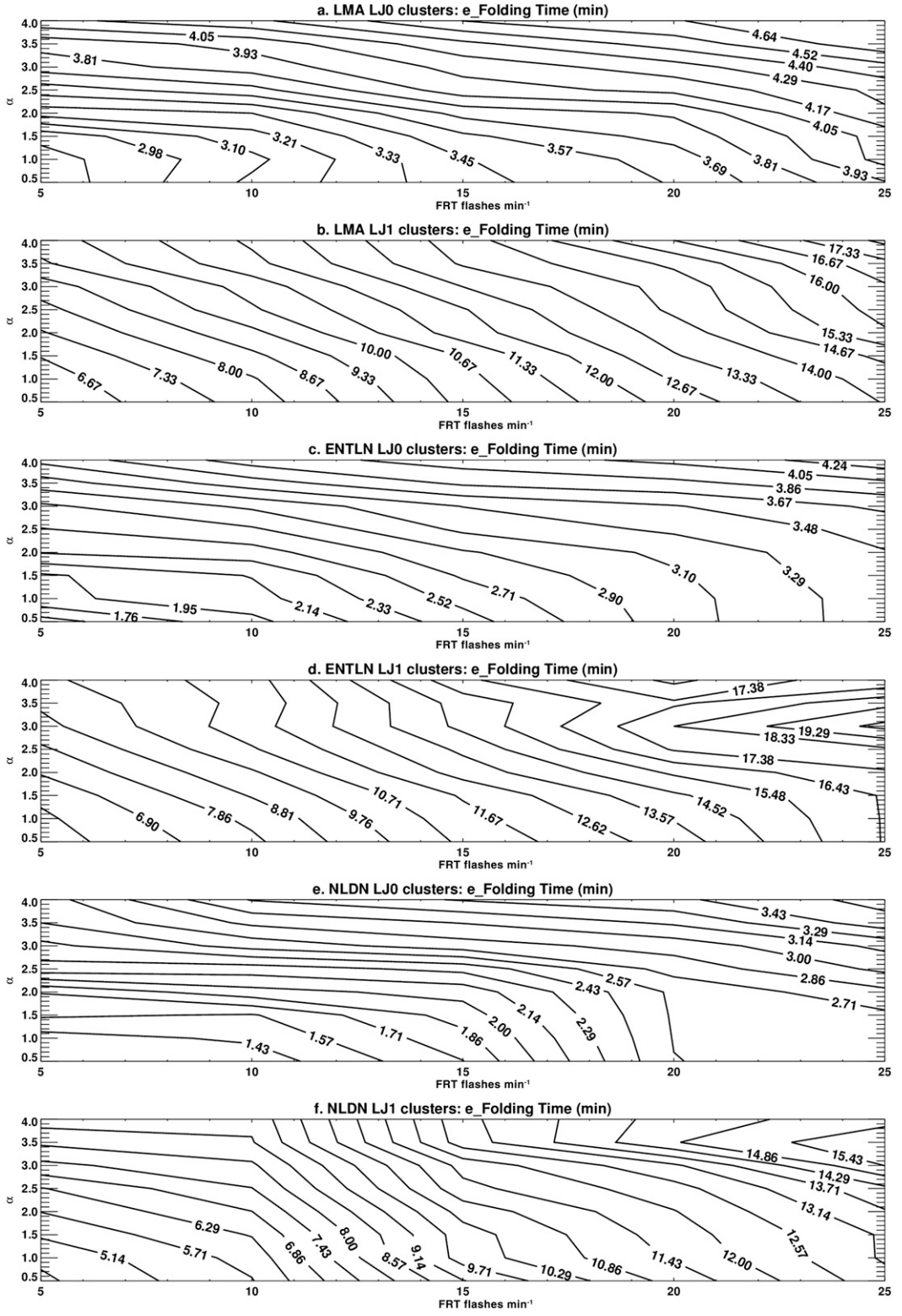

FIG. 3. Mean *e*-folding time (min) for LJ0/LJ1, as a function of FRT (*x* axis; flashes min^{-1}) and α (*y* axis) for (a),(b) LMA; (c),(d) ENTLN; and (e),(f) NLDN.

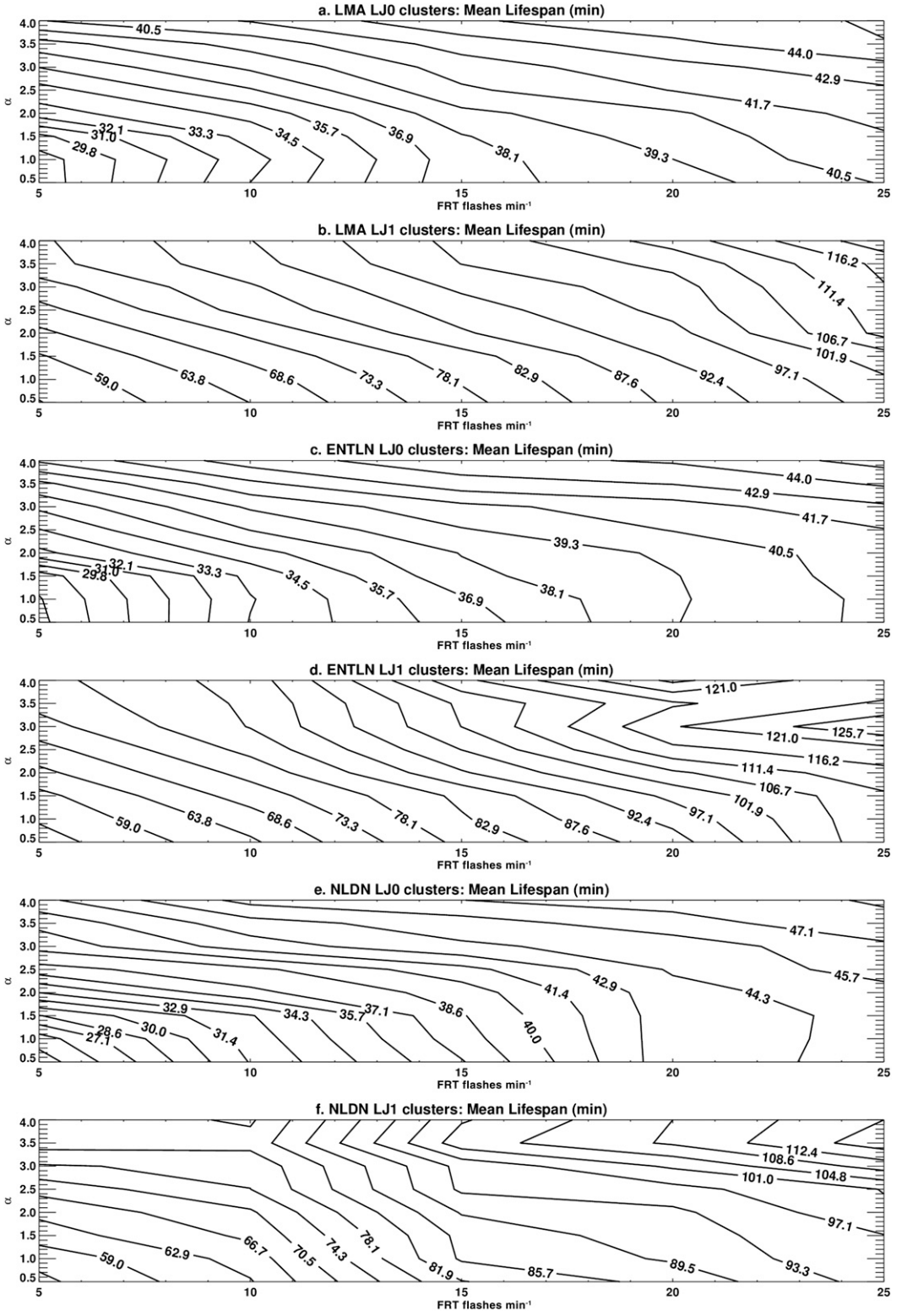

FIG. 4. Mean life span (min) for LJ0/LJ1, as a function of FRT (x axis; flashes min^{-1}) and α (y axis) for (a),(b) LMA; (c),(d) ENTLN; and (e),(f) NLDN.

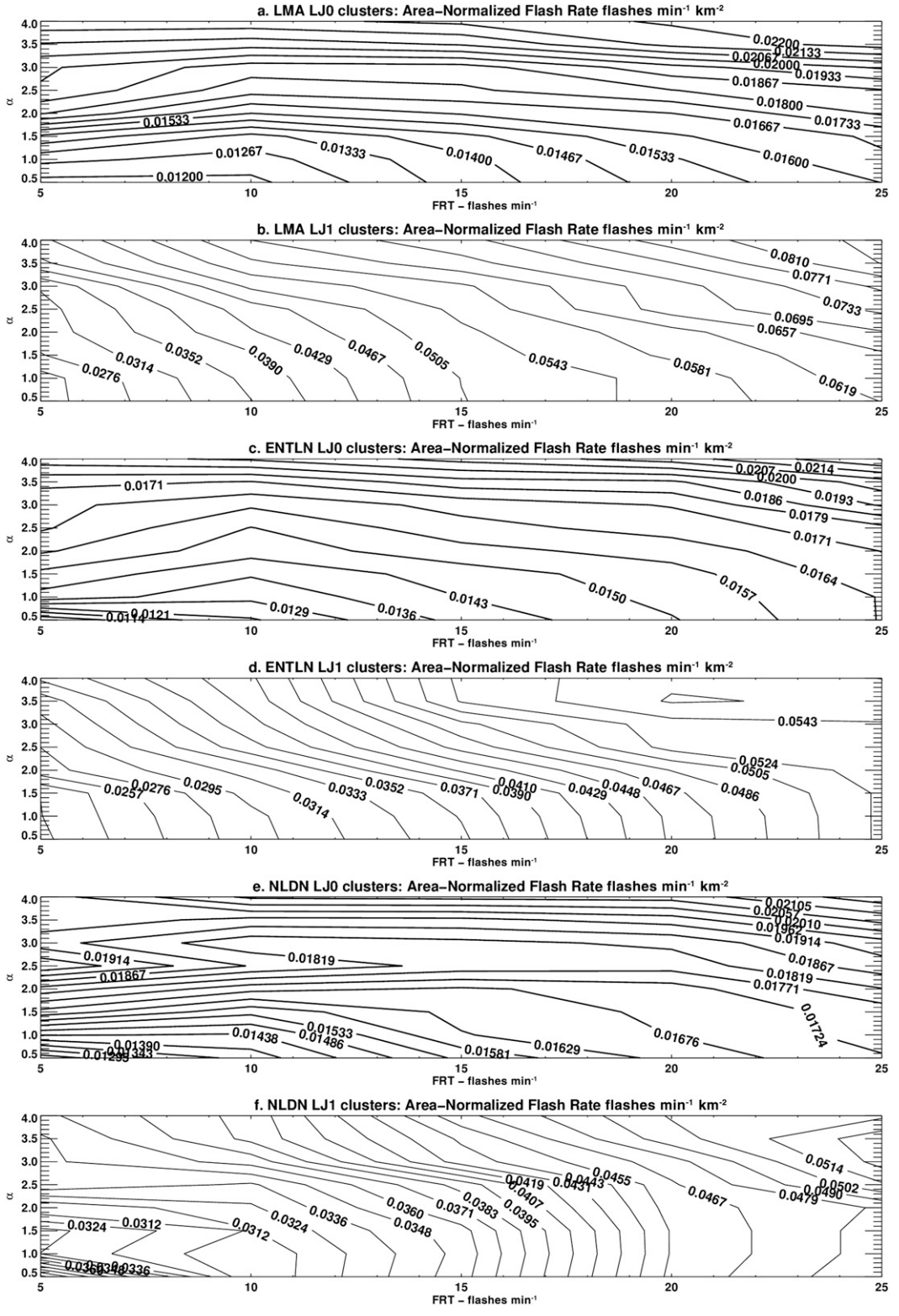

Fig. 5. Mean area-normalized flash rate (flashes $\mathrm{min}^{-1}\,\mathrm{km}^{-2}$) for LJ0/LJ1, as a function of FRT (x axis; flashes min^{-1}) and α (y axis) for (a),(b) LMA; (c),(d) ENTLN; and (e),(f) NLDN.

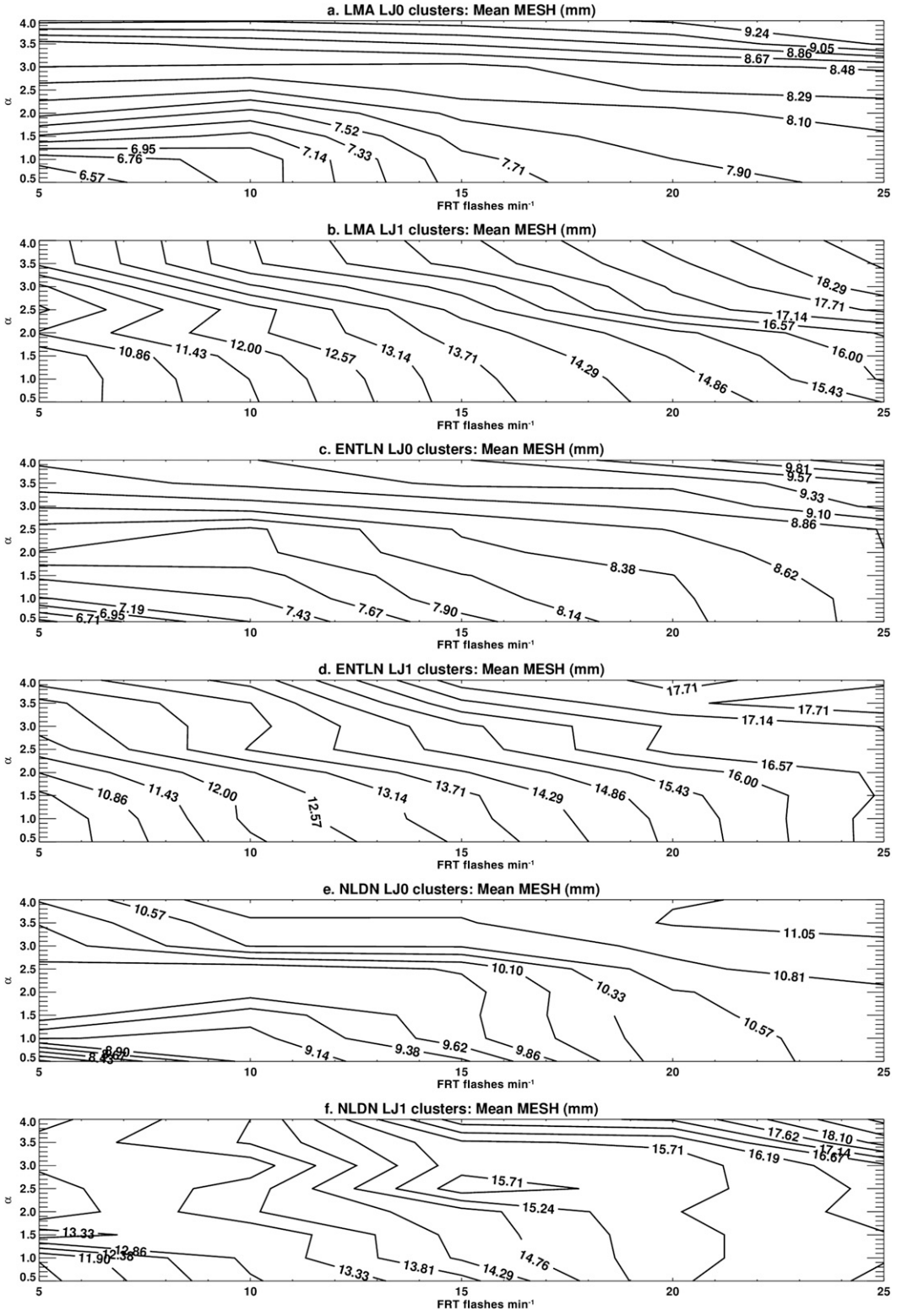

FIG. 6. Mean MESH (mm) for LJ0/LJ1, as a function of FRT (x axis; flashes min^{-1}) and α (y axis) for (a),(b) LMA; (c),(d) ENTLN; and (e),(f) NLDN.

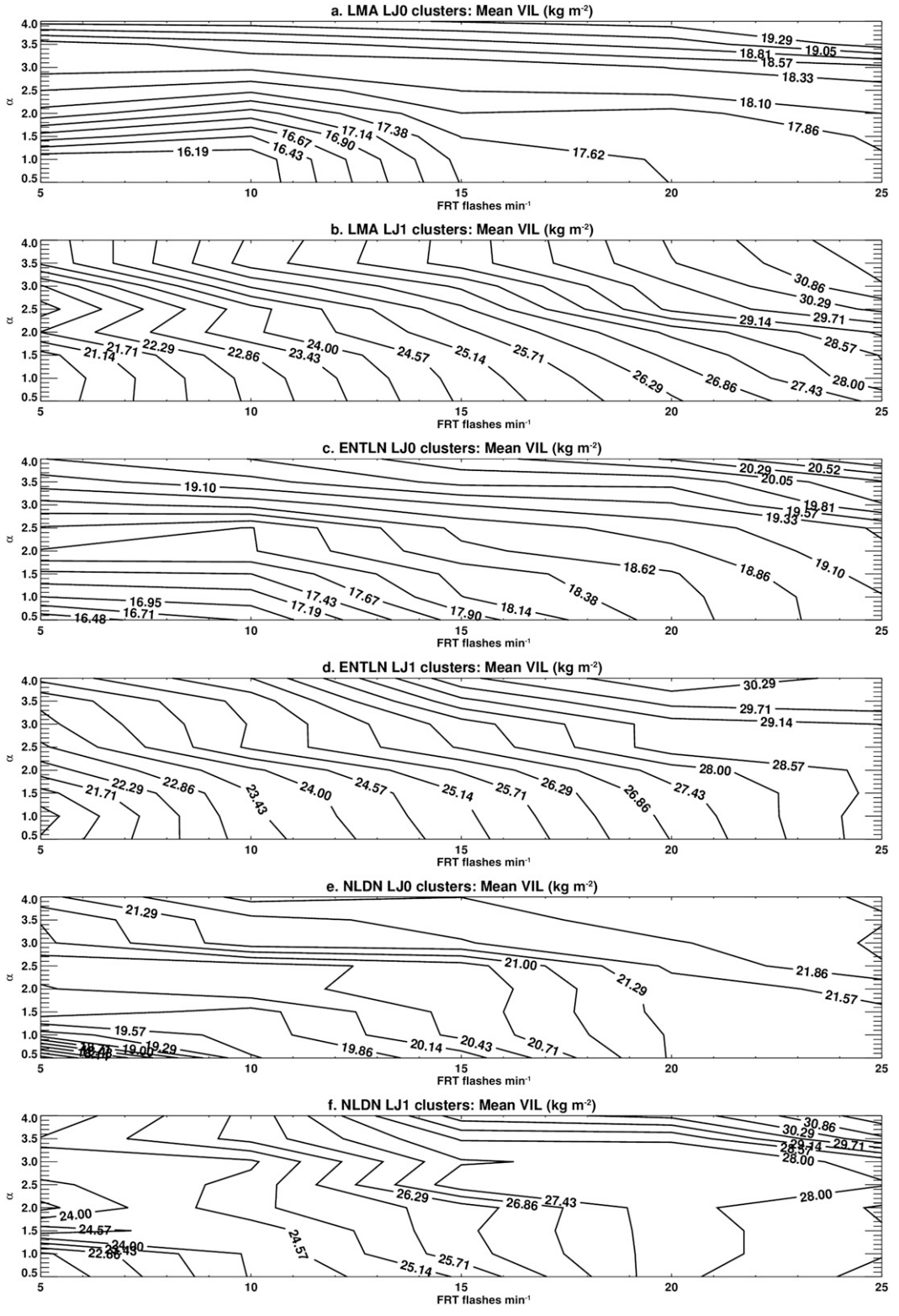

FIG. 7. Mean VIL (kg m^{-2}), for LJ0/LJ1, as a function of FRT (x axis; flashes min^{-1}) and α (y axis) for (a),(b) LMA; (c),(d) ENTLN; and (e),(f) NLDN.

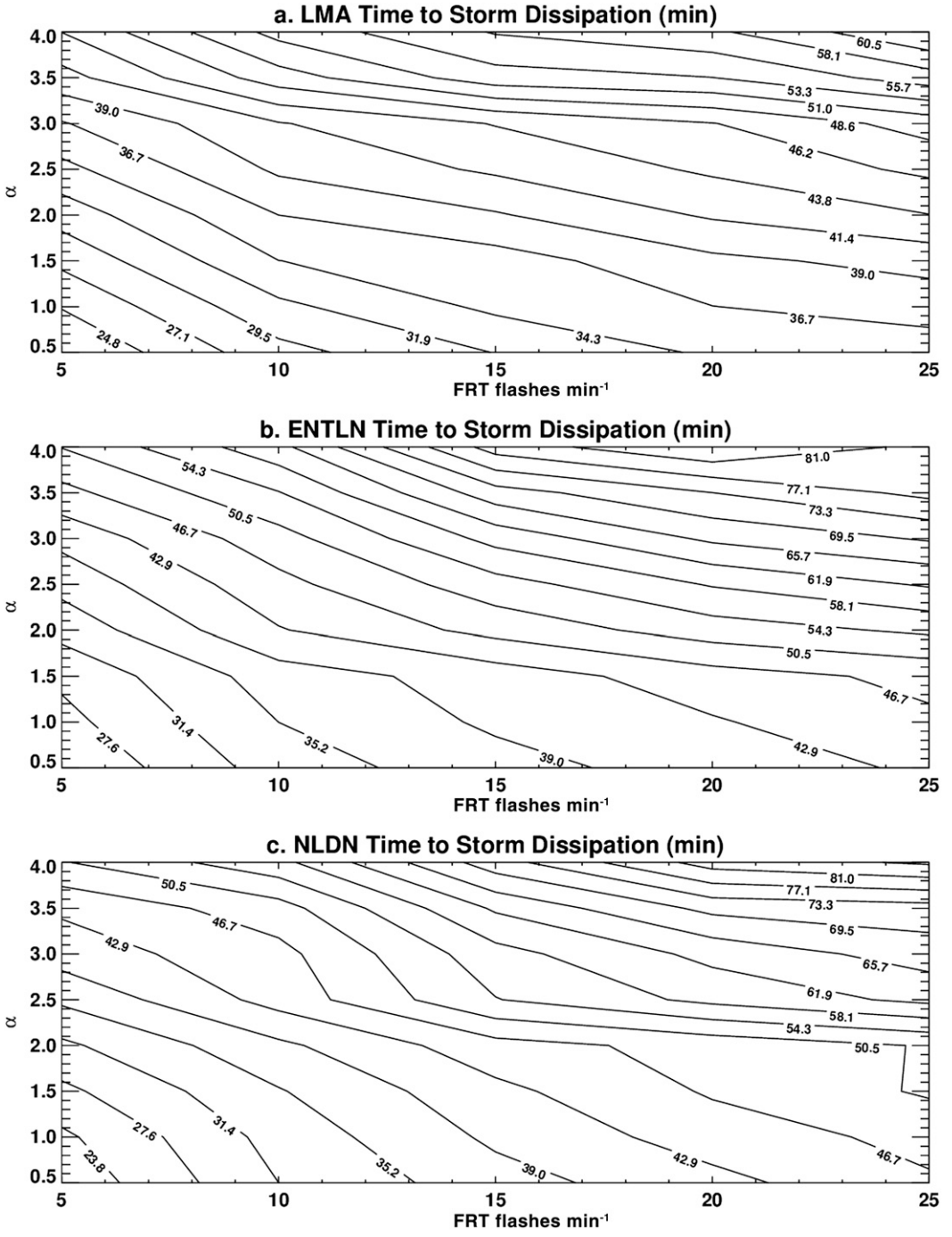

FIG. 8. Time elapsed until the storm dissipation for LJ1 (min) from (a) LMA, (b) ENTLN, and (c) NLDN, as a function of FRT (x axis; flashes min^{-1}) and α (y axis).

4. Conclusions

The observations herein indicate that the presence of an LJ has implications for a storm's dynamics, intensity, and evolution. The e-folding times are lower for the LJ1 clusters. For example, the e-folding times for the LJ1 at $\alpha = 2.0$ and FRT $= 15$ flashes min^{-1} are computed as ~12 min for LMA, 12.7 min for the ENTLN, and 11.5 min for the NLDN. Conversely, the e-folding times for the LJ0 for the same α and FRT values are consistently less than ~4.0 min for all three lightning detection systems. Through the enhanced updraft hypothesis, these findings indicate that the

presence of an LJ signals the storm's ability to sustain convection.

The study also documents that LJ1 clusters last longer and exhibit higher flash rates (area normalized), as well as larger MESH and VIL values, further corroborating previous studies that also suggest that the temporal total lightning variability is a dependable proxy for severe weather risk assessment (Williams 2001; Schultz et al. 2009, 2011; Rudlosky and Fuelberg 2013). In addition, the MESH values for the LJ1 clusters range from ~11 to 18 mm whereas the respective LJ0 values range from ~6.5 to 10 mm (Fig. 5). The mean values of VIL are ~18 kg m^{-2} for the LJ0 cases and ~25 kg m^{-2} for the LJ1 clusters.

The results throughout this analysis consistently suggest that there is no redundancy in the role of α and FRT in the LJ numerical implementation. This is shown by the increasing magnitudes of the implicated variables (e.g., *e*-folding time, MESH, flash rate, etc.; see Figs. 2–7) for LJ1 clusters increase as both α and FRT values also increase. Finally, the study offers further evidence that the presence and temporal coincidence of an LJ could be viewed as a proxy for the storm's expected dissipation. Typically, these values range between 20 and 60 min, depending on the LJ strength, with stronger jumps indicating more time until storm decay.

Ongoing efforts are exploring the value of the LJ as a component in operational severe weather watch/warning issuances (Schultz et al. 2014). The upcoming Geostationary Lightning Mapper (GLM) on board the GOES-R mission (Goodman et al. 2013) will provide continuous monitoring of total lightning activity across the Western Hemisphere. GLM will provide even greater detail on the linkage between temporal lightning variability and the storm evolution over areas where currently related information, including radar, is limited or nonexistent. Importantly, GLM will provide continuous coverage of total lightning over a large domain to evaluate this study on the global scale.

Acknowledgments. We acknowledge the support by the GOES-R System Program as part of the Proving Ground and Risk Reduction programs. The first and second authors also acknowledge the support by the UAH Individual Investigator Distinguished Research awards for 2014. CJS would like to acknowledge the NASA Pathways Intern Program, which provided the funding for support of this work. Sincere thanks to 1) Geoffrey Stano and the NASA Short-Term Prediction Research and Transition Center (SPoRT) for the NA LMA, 2) Earth Networks for the ENTLN data, 3) Vaisala for the NLDN data, 4) Donald R. MacGorman for the Oklahoma LMA data, and 5) Monte Bateman for the ENTLN processing. We would also like to extend our sincere thanks to the three anonymous reviewers who helped us improve this paper.

REFERENCES

Amburn, S., and P. Wolf, 1996: VIL density as a hail indicator. Preprints, *18th Conf. on Severe Local Storms,* San Francisco, CA, Amer. Meteor. Soc., 581–585.

Bowerman, B. L., and R. T. O'Connell, 1979: *Time Series and Forecasting: An Applied Approach.* Duxbury Press, 481 pp.

Bruning, E. C., and D. R. MacGorman, 2013: Theory and observations of controls on lightning flash size spectra. *J. Atmos. Sci.,* **70,** 4012–4029, doi:10.1175/JAS-D-12-0289.1.

Carey, L. D., and S. A. Rutledge, 2000: On the relationship between precipitation and lightning in tropical island convection: A C-band polarimetric radar study. *Mon. Wea. Rev.,* **128,** 2687–2710, doi:10.1175/1520-0493(2000)128<2687:TRBPAL>2.0.CO;2.

——, W. A. Petersen, and C. J. Schultz, 2009: A statistical framework for the development and evaluation of a lightning jump algorithm. Preprints, *Fourth Conf. on the Meteorological Applications of Lightning Data,* Phoenix, AZ, Amer. Meteor. Soc., P1.13. [Available online at https://ams.confex.com/ams/89annual/techprogram/paper_150768.htm.]

Chronis, T., E. Williams, E. Anagnostou, Walt Petersen, 2007: Lightning as a precursor of tropical cyclogenesis. *Eos, Trans. Amer. Geophys. Union,* **88,** 397, doi:10.1029/2007EO400001.

Cintineo, L. J., T. M. Smith, V. Lakshmanan, H. E. Brooks, and K. L. Ortega, 2012: An objective high-resolution hail climatology of the contiguous United States. *Wea. Forecasting,* **27,** 1235–1248, doi:10.1175/WAF-D-11-00151.1.

——, M. J. Pavolonis, J. M. Sieglaff, and D. T. Lindsey, 2014: An empirical model for assessing the severe weather potential of developing convection. *Wea. Forecasting,* **29,** 639–653, doi:10.1175/WAF-D-13-00113.1.

Cummins, K. L., and M. J. Murphy, 2009: An overview of lightning locating systems: History, techniques, and data uses, with an in-depth look at the U.S. NLDN. *IEEE Trans. Electromagn. Compat.,* **51,** 499–518, doi:10.1109/TEMC.2009.2023450.

——, E. A. Bardo, W. L. Hiscox, R. B. Pyle, and A. E. Pifer, 1995: NLDN '95: A combined TOA/MDF technology upgrade of the U.S. National Lightning Detection Network. *Proc. Int. Aerospace and Ground Conf. on Lightning and Static Electricity,* Williamsburg, VA, National Interagency Coordination Group of the National Atmospheric Electricity Hazards Protection Program, 1–15.

——, E. P. Krider, and M. Malone, 1998: The U.S. National Detection Network and applications of cloud-to-ground lightning data by electric power utilities. *IEEE Trans. Electromagn. Compat.,* **40,** 465–480, doi:10.1109/15.736207.

——, J. Cramer, C. Biagi, E. P. Krider, J. Jerauld, M. Uman, and V. Rakov, 2006: The U.S. National Lightning Detection Network: Post-upgrade status. Preprints, *Second Conf. on Meteorological Applications of Lightning Data,* Atlanta, GA, Amer. Meteor. Soc., 6.1. [Available online at https://ams.confex.com/ams/pdfpapers/105142.pdf.]

Deierling, W., and W. A. Petersen, 2008: Total lightning activity as an indicator of updraft characteristics. *J. Geophys. Res.,* **113,** D16210, doi:10.1029/2007JD009598.

Emersic, C., and C. P. R. Saunders, 2010: Further laboratory investigations into the relative diffusional growth rate theory of thunderstorm electrification. *Atmos. Res.,* **98,** doi:10.1016/j.atmosres.2010.07.011.

Gatlin, P., and S. J. Goodman, 2010: A total lightning trending algorithm to identify severe thunderstorms. *J. Atmos. Oceanic Technol.,* **27,** 3–22, doi:10.1175/2009JTECHA1286.1.

Goodman, S. J., D. E. Buechler, P. D. Wright, and W. D. Rust, 1988: Lightning and precipitation history of a microburst-producing storm. *Geophys. Res. Lett.,* **15,** 1185–1188, doi:10.1029/GL015i011p01185.

——, and Coauthors, 2005: The North Alabama Lightning Mapping Array: Recent severe storm observations and future prospects. *Atmos. Res.,* **76,** 423–437, doi:10.1016/j.atmosres.2004.11.035.

Goodman S., and Coauthors, 2013: The GOES-R Geostationary Lightning Mapper (GLM). *Atmos. Res.,* **125–126,** 34–49, doi:10.1016/j.atmosres.2013.01.006.

Greene, D. R., and R. A. Clark, 1972: Vertically integrated liquid water—A new analysis tool. *Mon. Wea. Rev.,* **100,** 548–552, doi:10.1175/1520-0493(1972)100<0548:VILWNA>2.3.CO;2.

Keene, K. M., P. T. Schlatter, J. E. Hales, and H. Brooks, 2008: Evaluation of NWS watch and warning performance related to tornadic events. Preprints, *24th Conf. on Severe Local Storms,* Savannah, GA, Amer. Meteor. Soc., P3.19. [Available online at https://ams.confex.com/ams/pdfpapers/142183.pdf.]

Kolodziej Hobson, A. G. K., V. Lakshmanan, T. M. Smith, and M. Richman, 2012: An automated technique to categorize storm type from radar and near-storm environment data. *Atmos. Res.,* **111,** 104–113, doi:10.1016/j.atmosres.2012.03.004.

Koshak, W. J., and Coauthors, 2004: North Alabama Lightning Mapping Array (LMA): VHF source retrieval algorithm and error analyses. *J. Atmos. Oceanic Technol.,* **21,** 543–558, doi:10.1175/1520-0426(2004)021<0543:NALMAL>2.0.CO;2.

Krehbiel, P. R., 2008: The DC Lightning Mapping Array. Preprints, *Third Conf. on Meteorological Applications of Lightning Data,* New Orleans, LA, Amer. Meteor. Soc., 3.2. [Available online at https://ams.confex.com/ams/88Annual/techprogram/paper_129095.htm.]

Lakshmanan, V., and T. Smith, 2009: Data mining storm attributes from spatial grids. *J. Atmos. Oceanic Technol.,* **26,** 2353–2365, doi:10.1175/2009JTECHA1257.1.

——, ——, G. J. Stumpf, and K. Hondl, 2007: The Warning Decision Support System–Integrated Information. *Wea. Forecasting,* **22,** 596–612, doi:10.1175/WAF1009.1.

——, K. Hondl, and R. Rabin, 2009: An efficient, general-purpose technique for identifying storm cells in geospatial images. *J. Atmos. Oceanic Technol.,* **26,** 523–537, doi:10.1175/2008JTECHA1153.1.

Liu, C., and S. Heckman, 2011: The application of total lightning detection and cell tracking for severe weather prediction. *Proc. Fifth Conf. on the Meteorological Applications of Lightning Data,* Seattle, WA, Amer. Meteor. Soc., 8.2. [Available online at https://ams.confex.com/ams/91Annual/webprogram/Paper183895.html.]

MacGorman, D. R., and C. D. Morgenstern, 1998: Some characteristics of cloud to ground lightning in mesoscale convective systems. *J. Geophys. Res.,* **103,** 14 011–14 023, doi:10.1029/97JD03221.

——, and Coauthors, 2008: TELEX: The Thunderstorm Electrification and Lightning Experiment. *Bull. Amer. Meteor. Soc.,* **89,** 997–1013, doi:10.1175/2007BAMS2352.1.

McCaul, E. W., J. Bailey, J. Hall, S. J. Goodman, R. Blakeslee, and D. E. Buechler, 2005: A flash clustering algorithm for North Alabama Lightning Mapping Array data. Preprints, *Conf. on Meteorological Applications of Lightning Data,* San Diego, CA, Amer. Meteor. Soc., 5.2. [Available online at https://ams.confex.com/ams/pdfpapers/84373.pdf.]

Murphy, M. J., and A. Nag, 2014: Enhanced cloud lightning performance of the U.S. National Lightning Detection Network following the 2013 upgrade. *23rd Int. Lightning Detection Conf./5th Int. Lightning Meteorology Conf.,* Tucson, AZ, Vaisala. [Available online at http://www.vaisala.com/en/events/ildcilmc/Pages/ILDC-2014-archive.aspx.]

Rudlosky, S. D., and H. E. Fuelberg, 2010: Pre- and postupgrade distributions of NLDN reported cloud-to-ground lightning characteristics in the contiguous United States. *Mon. Wea. Rev.,* **138,** 3623–3633, doi:10.1175/2010MWR3283.1.

——, and ——, 2013: Documenting storm severity in the mid-Atlantic region using lightning and radar information. *Mon. Wea. Rev.,* **141,** 3186–3202, doi:10.1175/MWR-D-12-00287.1.

Saunders, C. P. R., 1993: A review of thunderstorm electrification processes. *J. Appl. Meteor.,* **32,** 642–655, doi:10.1175/1520-0450(1993)032<0642:AROTEP>2.0.CO;2.

——, H. Bax-Norman, C. Emersic, E. E. Avila, and N. E. Castellano, 2006: Laboratory studies of the effect of cloud conditions on graupel/crystal charge transfer in thunderstorm electrification. *Quart. J. Roy. Meteor. Soc.,* **132,** 2653–2673, doi:10.1256/qj.05.218.

Schultz, C. J., W. A. Petersen, and L. D. Carey, 2009: Preliminary development and evaluation of lightning jump algorithms for the real-time detection of severe weather. *J. Appl. Meteor. Climatol.,* **48,** 2543–2563, doi:10.1175/2009JAMC2237.1.

——, ——, and ——, 2011: Lightning and severe weather: A comparison between total and cloud-to-ground lightning trends. *Wea. Forecasting,* **26,** 744–755, doi:10.1175/WAF-D-10-05026.1.

——, L. D. Carey, E. V. Schultz, R. J. Blakeslee, and S. J. Goodman, 2014: Physical and dynamical linkages between lightning jumps and storm conceptual models. *Proc. 15th Int. Conf. on Atmospheric Electricity,* Norman, OK, IUGG/IAMAS. [Available online at http://www.nssl.noaa.gov/users/mansell/icae2014/preprints/Schultz_246.pdf.]

Stumpf, G. J., T. M. Smith, and J. Hocker, 2004: New hail diagnostic parameters derived by integrating multiple radars and multiple sensors. Preprints, *22nd Conf. on Severe Local Storms,* Hyannis, MA, Amer. Meteor. Soc., P7.8. [Available online at https://ams.confex.com/ams/pdfpapers/81451.pdf.]

Takahashi, T., 1978: Riming electrification as a charge generating mechanism. *J. Atmos. Sci.,* **35,** 1536–1548, doi:10.1175/1520-0469(1978)035<1536:REAACG>2.0.CO;2.

Thomas, R., P. Krehbiel, W. Rison, J. Harlin, T. Hamlin, and N. Campbell, 2003: The LMA flash algorithm. Proc. *12th Int. Conf. on Atmospheric Electricity,* Versailles, France, Int. Commission on Atmospheric Electricity, 655–656.

——, ——, ——, S. J. Hunyady, W. P. Winn, T. Hamlin, and J. Harlin, 2004: Accuracy of the Lightning Mapping Array. *J. Geophys. Res.,* **109,** D14207, doi:10.1029/2004JD004549.

Trapp, R. J., D. M. Wheatly, N. T. Atkins, and R. W. Przybylinkski, 2006: Buyer beware: Some words of caution on the use of severe wind reports in postevent assessment and research. *Wea. Forecasting,* **21,** 408–415, doi:10.1175/WAF925.1.

Uman, M. A., 1987: *The Lightning Discharge.* Academic Press, 183 pp.

Williams, E. R., 2001: The electrification of severe storms. *Severe Convective Storms, Meteor. Monogr.,* No. 50, Amer. Meteor. Soc., 527–561.

——, and Coauthors, 1999: The behavior of total lightning activity in severe Florida thunderstorms. *Atmos. Res.,* **51,** 245–265, doi:10.1016/S0169-8095(99)00011-3.

Witt, A., M. D. Eilts, G. J. Stumpf, J. T. Johnson, E. D. Mitchell, and K. W. Thomas, 1998: An enhanced hail detection algorithm for the WSR-88D. *Wea. Forecasting,* **13,** 286–303, doi:10.1175/1520-0434(1998)013<0286:AEHDAF>2.0.CO;2.